A Small 4-wheeler EV Propulsion System Using DTC Controlled Induction Motor

Deepak Ronanki, A Hemasundar and P Parthiban, *Member, IEEE*

***Abstract*—With the increasing need of electric vehicles (EV), necessary development is required to get reliable, efficient and economical drives for electric propulsion. Electric propulsion system using Induction Motor drive (IM) is becoming so popular because of its reliability, technological maturity and low cost. Field Orientation Control (FOC) is so popular in controlling the IM, but it has disadvantages like sensitive to parametric variation, external disturbance, load variation and also algorithm takes more time for execution, hence it requires a very fast microprocessor with high millions of instructions per second (MIPS) for implementation. In this paper, IM is controlled by using Direct Torque Control (DTC) technique because of its simple configuration and gives quick response. The mathematical model takes into account of the inverter, IM dynamics and vehicle aerodynamics. In this paper, the response of the IM with DTC for EV load for driving cycle consists of starting, acceleration, constant speed and deceleration modes are explained and validated using MATLAB/SIMULINK.**

***Index Terms*—Direct Torque Control (DTC), Electric Vehicle (EV), Induction Motor (IM), MATLAB**

I. Introduction

IN developing countries like India, urban transportation is the prime issue on environmental and economic aspects. Air pollution, global warming, the rapid depletion of the earth' s petroleum resources and also rapid increase in fuel rate are the major concerns, so there is a need to develop an efficient, clean and safe transportation. EV is only an alternative to replace conventional Internal Combustion Engine (ICE) for urban transportation since it has advantages like high efficiency, free from petroleum, absence of emissions, quiet and smooth operation [1].

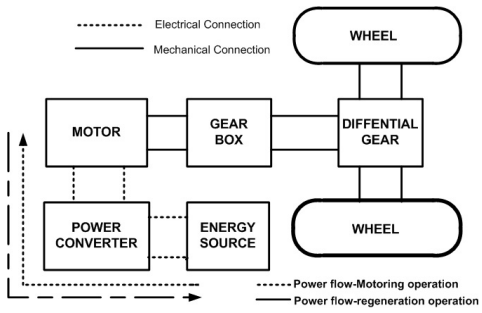

Fig. 1. Basic electrical composition of the 4-wheeler EV

Deepak Ronanki is a post graduate student of Electrical and Electrical Engineering, National Institute of Technology Karnataka, Surathkal, India-575025, Email: deepuronnitk@gmail.com.

A hemasundar is a post graduate student of Electrical and Electrical Engineering, National Institute of Technology Karnataka, Surathkal, India-575025.

Parthiban P is with the Department of Electrical and Electronics Engineering, National Institute of Technology Karnataka, surathkal, Karntaka India-575025, Email:parthdee@nitk.ac.in.

EV system consists of electric motor, power converter, electronic controllers, energy source, transmission device, and wheels as shown in Fig.1. Based on the control inputs from the accelerator and brake pedals, the vehicle controller provides proper control signals to the electronic power converter, which functions to regulate the power flow between the electric motor and energy source [2].

Table I shows the comparison between DC, IM, PMSM and SRM for EV application, each of them is graded from 1 to 5 points, where 5 points means the best. The comparative study has revealed that the induction motor drives are preferred for EV propulsion, due to their low cost, robust, high reliability, established converter, wide speed range, manufacturing technology, low torque ripple, less acoustic noise, absence of position sensors and free from maintenance [4].

TABLE I
Comparison Between Different Machines [3]

Characteristics	DC	IM	PMSM	SRM
Power Density	2.5	3.5	5	3.5
Efficiency	2.5	3.5	5	3.5
Controllability	5	5	4	3
Reliability	3	5	4	5
Technological maturity	5	5	4	4
Cost	4	5	3	4
$\sum$ Total	22	27	25	23

Generally FOC is used for improving the dynamic performance of induction motor drives for electric vehicle propulsion. However in FOC, in order to decouple the interaction between flux control and torque control uses quite complicated coordinate transformations to provide fast torque control of an induction motor. Hence the computation algorithm takes more time for execution and its implementation usually requires a fast micro processor with MIPS. It is also sensitive to the system variations and inadequate rejection of external disturbances and load changes.

Several researchers already used DTC technique for controlling IM as electric propulsion system because it can provide fast torque control and doesn't require heavy on-line computation time. The Direct Torque Control (DTC) was proposed by M.Depenbrock [5] and I.Takahashi [6] in 1985. Some of the recent work for controlling IM for EV application is in [7]-[10]. In this paper, analytical expressions are derived for DTC of IM with EV load. In this paper, section II is devoted to a modeling of vehicle load. In section III, explains about system description which includes the modeling of IM, Inverter and different blocks in DTC.

ISBN: 978-988-19252-8-2
ISSN: 2078-0958 (Print); ISSN: 2078-0966 (Online)

Simulation results for DTC of IM in acceleration mode, constant speed mode and deceleration modes are presented in section IV.

II. Vehicle Model

The straight line motion of a vehicle can be approximately modeled using following equation [1]

$$m\frac{dv}{dt} = F_t - \Sigma F_r \tag{1}$$

where,
v=speed of the vehicle (m/s)
m=mass of the vehicle (kg)
F_t=Tractive effort of the vehicle (N)
F_r are the forces resisting vehicle's motion. These include:

- Force due to rolling friction of the tyres with the road surface given by

$$F_{friction} = \mu_r mgcos\theta \tag{2}$$

where, μ_r=coefficient of rolling friction, g=9.8 m/s^2=gravitational acceleration.

- Aerodynamic drag as vehicle tries to move through air given by

$$F_{drag} = \frac{1}{2}C_d\rho Av^2 \tag{3}$$

where, C_d=coefficient of drag, A=aerodynamic reference area (m^2), ρ=density of air (1.2 kg/m^3 at 20^oc).

- Grading resistance when vehicle tries to climb up or down the slope. The mass of a vehicle creates component given by

$$F_{gradient} = mgsin\theta \tag{4}$$

In case of electric vehicle, the relation between vehicle speed to motor speed (rpm) is given by

$$v = \frac{\pi N_m r}{30G\eta_t} \tag{5}$$

where, r=wheel radius, G=gear transmission ratio, η_t=transmission efficiency (0.97 to 0.98).
Substituting all above equations in equation (1), the overall dynamic equation of motion of the vehicle on flat road is given in [1] is

$$(m + \frac{J}{r^2})\frac{dv}{dt} = \frac{T_m}{r} - \mu_r mg - \frac{1}{2}C_d\rho Av^2 \tag{6}$$

where, J=moment of inertia of vehicle, it can be accounted for by increasing the mass by 5% [11].
Using the equations (5 & 6), the vehicle load is modeled in the Matlab/simulink. The power rating (P_m) of the motor can be given by

$$P_m = F_t v = T_m\frac{2\pi N_m}{60} \tag{7}$$

For the max speed of 80 kmph, the motor rating is obtained as 2.1 kW

III. System Description

The complete IM drive system is as shown in Fig 2. It includes IM, Inverter, torque and flux hysteresis controller, optimal switching table and estimation of torque and flux. Each block in this system is modeled separately and integrated together.

TABLE II
Vehicle parameters used for the study [12]

Parameter	Value
Mass of the vehicle (m)	500 kg
Aerodynamic area (A)	2.4 m^2
Aero dynamic drag (C_d)	0.51
Rolling resistance (μ_r)	0.015
Wheel radius (r)	0.26m
Gear Transmission Ratio (G)	10
Transmission Efficiency (η_t)	0.98

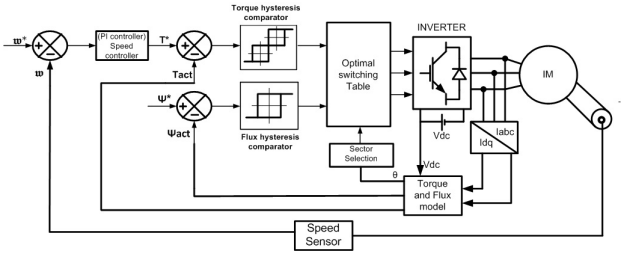

Fig. 2. Block diagram of closed loop Direct Torque Control of IM

A. Modeling of Induction Motor [13]

The machine model equations in general reference frame are given below, where g denotes the general reference frame.

$$v_s^g = i_s^g R_s + j\omega_g\psi_s^g + p\psi_s^g \tag{8}$$

$$0 = i_r^g R_r + j(\omega_g - \omega_g)\psi_r^g + p\psi_r^g \tag{9}$$

$$\psi_s^g = L_s i_s^g + L_m i_r^g \tag{10}$$

$$\psi_r^g = L_r i_r^g + L_m i_s^g \tag{11}$$

The developed electromagnetic torque T_{em} equation can be given as

$$T_{em} = \frac{3P}{4}(\psi_{sd}^g i_{sq}^g - \psi_{sq}^g i_{sd}^g) \tag{12}$$

For stationery reference frame the machine model equations will be modified to the following equations, where axis is aligned with the magnetic axis of the stator coil, R.

$$v_s^\alpha = i_s^\alpha R_s + j\omega_\alpha\psi_s^\alpha + p\psi_s^\alpha \tag{13}$$

$$0 = i_r^\alpha R_r + j(\omega_\alpha - \omega_\alpha)\psi_r^\alpha + p\psi_r^\alpha \tag{14}$$

$$\psi_s^\alpha = L_s i_s^\alpha + L_m i_r^\alpha \tag{15}$$

$$\psi_r^\alpha = L_r i_r^\alpha + L_m i_s^\alpha \tag{16}$$

Where (ψ_s^α, ψ_r^α) are the stator and rotor flux linkages respectively. From Eq. (15) rotor current can be derived as

$$i_r^\alpha = \frac{(\psi_s^\alpha - L_s i_s^\alpha)}{L_m} \tag{17}$$

Combining Eq. (15) and (16)

$$\psi_s^\alpha = \frac{L_m}{L_r}\psi_r^\alpha + L_s^* i_s^\alpha \tag{18}$$

where $L_s^* = \frac{L_s L_r - L_m^2}{L_r}$
And stator current can be expressed as

$$i_s^\alpha = \frac{\psi_s^\alpha}{L_s^*} - (\frac{L_m}{L_r L_s^*})\psi_s^\alpha \tag{19}$$

ISBN: 978-988-19252-8-2
ISSN: 2078-0958 (Print); ISSN: 2078-0966 (Online)

The developed electromagnetic torque T_{em} equation can be given as

$$T_{em} = \frac{3P}{4}\frac{L_m}{L_r L_s}(\psi_s^{\alpha} \times \psi_s^{\alpha}) \tag{20}$$

$$T_{em} = \frac{3P}{4}\frac{L_m}{L_r L_s}(|\psi_s^{\alpha}||\psi_s^{\alpha}|sin\alpha) \tag{21}$$

where $\alpha = \delta_s - \delta_r$ denotes the angle between them while rotating in synchronous speed.

The mechanical torque equation can be given as

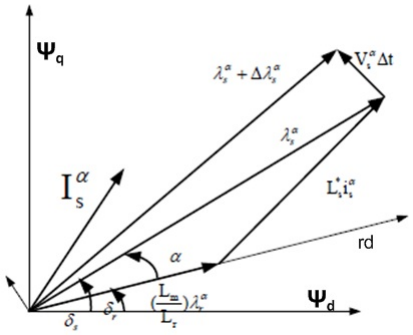

Fig. 3. Phasor diagram of stator and rotor flux linkage space vector

$$T_{em} - T_L = J\frac{d\omega}{dt} + B\omega \tag{22}$$

B. Inverter Modeling

Fig.4 shows the inverter which supplies the input voltage for the three phases of IM assuming that it is star connected. Each phase leg comprises of two power semiconductor devices.

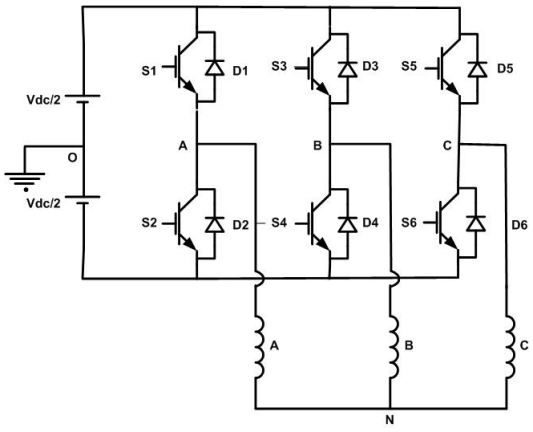

Fig. 4. Three phase IGBT based Inverter

$$V_{Ao} = (S_1) * \frac{V_{dc}}{2} - (S_6) * \frac{V_{dc}}{2} \tag{23}$$

$$V_{Bo} = (S_3) * \frac{V_{dc}}{2} - (S_4) * \frac{V_{dc}}{2} \tag{24}$$

$$V_{Co} = (S_5) * \frac{V_{dc}}{2} - (S_2) * \frac{V_{dc}}{2} \tag{25}$$

where V_{Ao}, V_{Bo} & V_{Co} are pole voltages

$$V_{AN} = \frac{2}{3}V_{Ao} - \frac{1}{3}V_{Bo} - \frac{1}{3}V_{Co} \tag{26}$$

Similarly for the other phases V_{BN} & V_{CN} where V_{AN},V_{BN} and V_{CN} are line-neutral voltages and V_{dc} is dc-link voltage Here we assumed switch-on state for upper switches is treated as 1 and lower switches as -1.

C. Torque and Flux hysteresis comparators

In this block, the reference and estimated values of torque and flux linkage vector are compared. If the reference torque is larger than the actual value, the comparator output as state 1 or otherwise -1. If the reference flux is larger than actual value, the comparator output state 1 or otherwise 0.

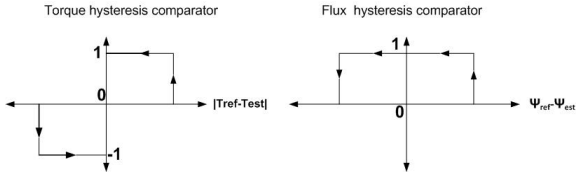

Fig. 5. Torque and Hysteresis Comparators

D. Optimal switching Table

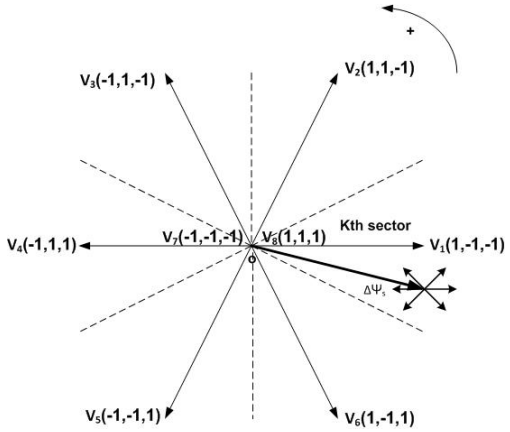

Fig. 6. Definition of voltage vectors and sectors

The estimated torque and flux values are compared with the reference values, the error is compared in hysteresis comparator and the output of the comparators along with the flux vector angle (θ) are together used in switching table to determine the appropriate voltage vector. The voltage vector obtained from the switching table is then applied to the Voltage Source Inverter (VSI). The phase voltages can be represented in switch states and space vector for voltage as

$$v_s = \frac{2}{3}V(S_a + S_b \exp j\frac{2\Pi}{3} + S_c \exp -j\frac{2\Pi}{3}) \tag{27}$$

Where v_s is the primary voltage space vector, S_a, S_b and S_c represent three-phase switching states.

There are six active vectors V_1 to V_6 which are apart from 60^o in space and the two zero voltage vectors V_0 and V_7 are located in the center of the space-vector plane. For a stator flux space vector that lies in the k^{th} sector, the voltage vectors v_k, v_{k+1} and v_{k-1} are chosen to increase the magnitude of the flux v_{k+2}, v_{k-2} and v_{k-3} can be chosen to decrease the flux magnitude [13]. In general, switching table is shown in Fig.7.

ISBN: 978-988-19252-8-2
ISSN: 2078-0958 (Print); ISSN: 2078-0966 (Online)

$T\uparrow\ \psi\uparrow$	$T\uparrow\ \psi\downarrow$	$T\downarrow\ \psi\uparrow$	$T\downarrow\ \psi\downarrow$
V_{k+1}	V_{k+2}	V_{k-1}	V_{k-2}

Fig. 7. Switching Table

E. Torque and Flux estimator

In order to determine the actual torque and flux linkage, flux and torque estimators are used. The three-phase variables (abc) are transformed into d-q axes by the following equation.

$$\begin{bmatrix} f_d \\ f_q \end{bmatrix} = \begin{bmatrix} \frac{2}{3} & \frac{-1}{3} & \frac{-1}{3} \\ 0 & \frac{1}{\sqrt{3}} & \frac{-1}{\sqrt{3}} \end{bmatrix} \begin{bmatrix} f_a \\ f_b \\ f_c \end{bmatrix} \tag{28}$$

where f can be voltage, current and flux linkages.
The stator flux linkage in d-q axes are estimated by:

$$\psi_{ds} = \int (v_{ds} - R_s i_{ds}) dt \tag{29}$$

$$\psi_{qs} = \int (v_{qs} - R_s i_{qs}) dt \tag{30}$$

The flux linkage phasor can be given as

$$\psi_s = \sqrt{\psi_{ds}^2 + \psi_{qs}^2} \tag{31}$$

$$\theta = tan^{-1}(\frac{\psi_{qs}}{\psi_{ds}}) \tag{32}$$

The location of the stator flux linkage vector is determined by equations (31) and (32). This angle can choose an appropriate set of vectors depending on the flux location.

The electromagnetic torque can be estimated as

$$T_{est} = \frac{3}{2} P(\psi_{ds} i_{qs} - \psi_{qs} i_{ds}) \tag{33}$$

TABLE III
MOTOR PARAMETERS USED IN THE SIMULATION

Parameter	Value
Motor rating (P)	$2.1kW$
Stator resistance (R_s)	7.83Ω
Rotor resistance(R_r)	7.55Ω
Stator self inductance (L_s)	.4751H
Rotor self inductance (L_r)	.4751H
Mutual Inductance(L_m)	.4535H
Moment of inertia (J in $kg-m^2$)	.06
No of poles (P)	4

IV. Simulation Results and Discussion

The DTC of IM has been simulated in Matlab/Simuink using basic simulink blocks. The simulation parameters have been given in Table III. Fig.8 shows the stator flux vector trajectory in d-q plane.

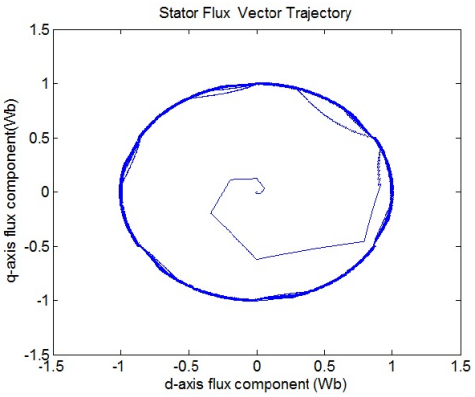

Fig. 8. Stator flux vector trajectory in d-q plane

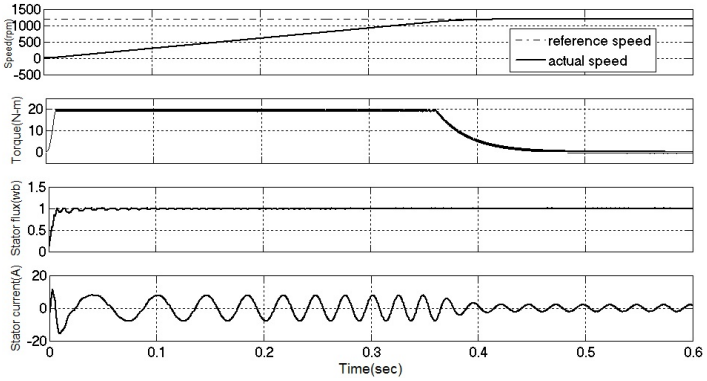

Fig. 9. Dynamic Response of IM when reference speed is 1200 rpm at No load

A. Dynamic response of IM at No load

This mode is also called free acceleration mode. Fig. 9 shows simulated waveforms of rotor speed, torque, stator flux and stator current when motor is at no-load. Fig. 9 shows that at time of starting (i.e from 0 to 1200 rpm) the motor draws an inrush current. At the time of starting, motor current has some distortion and after that three phase motor currents are close to sinusoidal and we can observe that the variation of the frequency of the currents as speed changes from zero to the nearly rated speed of the motor i.e 1200 rpm. Once the motor reaches to rated speed, motor has to supply power only to the load.

B. Dynamic response of IM during load variation at constant speed

Fig. 10 shows that vehicle is loaded from 0 N-m to (12 N-m) at constant speed of 1200 rpm. Loading can be done by use of external step source which change from 0 to 12 at 0.7 sec. The developed motor torque simply follows the reference value and it indicates that control is extremely fast. During loading, speed changed from 1200 rpm to 1140 rpm due to change of load from 0 to 12 N-m and also it draws more current than at No-load.

C. Dynamic Response of IM during deceleration

Fig.11 shows the transient response of vehicle motor during deceleration. When the IM is slowed down at 0.6 sec i.e from 1200 rpm to 600 rpm, a negative torque is

ISBN: 978-988-19252-8-2
ISSN: 2078-0958 (Print); ISSN: 2078-0966 (Online)

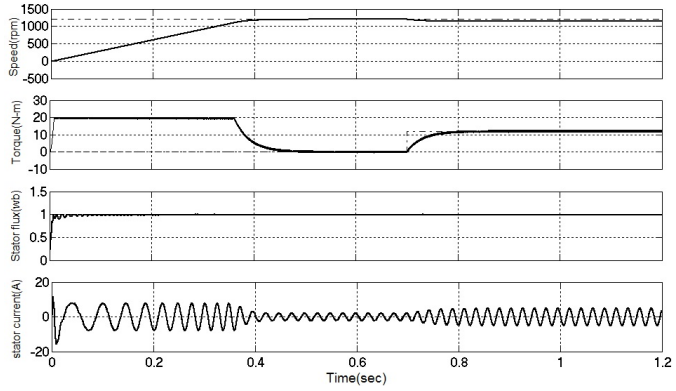

Fig. 10. Transient response of IM when step change in load from $T_L = 0$N-m to $T_L = 12$N-m

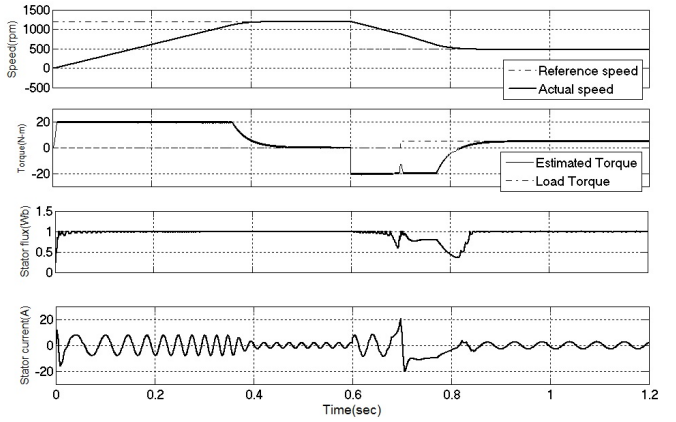

Fig. 11. Dynamic response of IM during deceleration mode

applied to the EV, it behaves as a electric generator which can produce electrical power back to source. This energy is utilized or stored in energy sources like batteries. we can also observe that IM currents during acceleration and deceleration are maximum. Fig. 11 shows that the IM currents are approximately near to sinusoidal and we can observe that the variation of the frequency of the currents as speed changes from 1200 rpm to 600 rpm at 0.6 second. This mode shows the behavior of reversal of a phase current during regenerative braking operation.

D. Dynamic response of IM during reverse rotation

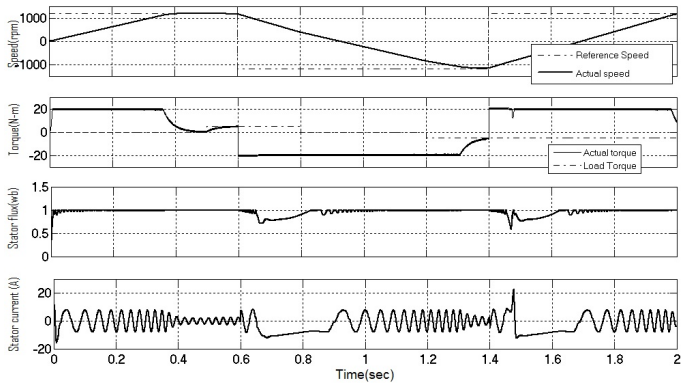

Fig. 12. Dynamic response of IM during reverse rotation

Fig. 12 shows that phase sequence reversal of motor currents when the direction of rotation is reversed from (1200 rpm to - 1200 rpm at 0.6 second) and (-1200 rpm to 1200 rpm at 1.6 second) and also shows the variation of the frequency of the currents.

E. Dynamic behavior of IM on application of vehicle load

Fig.13 shows the transient response of motor when the electric vehicle load is applied. The vehicle load parameters are given in Table II. The electromagnetic torque is able to track the vehicle load torque efficiently. From Fig. 9-13, we can be observe that torque response is very rapid especially during the starting stage due to the fact that stator flux is controlled while torque takes some time to reach its value. The result shows that the controller works very effectively and output simply follows the given reference. The results show that DTC will have quick response and flexible in control and best suited for the vehicle application.

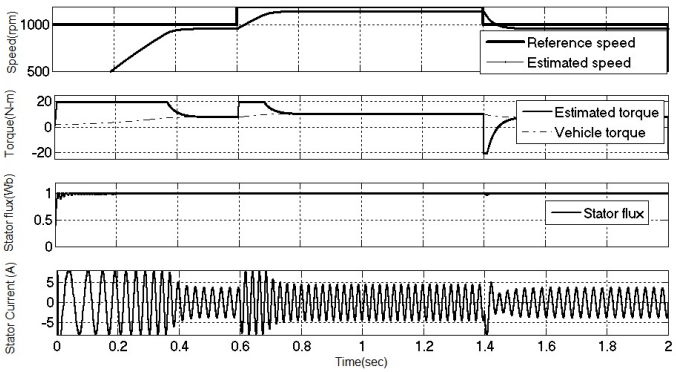

Fig. 13. Dynamic behavior of IM on application of vehicle load

V. Conclusion

The present paper shows the comparative study of traction motors used in electric vehicle, in which IM is best suited for the electric vehicle application. In this paper, the mathematical model of VSI, IM, each block in DTC of IM has been explained in detail. Analytical expressions for VSI fed IM with DTC and combined the vehicle aerodynamics are derived and validated using MATLAB/SIMULINK by using only basic simulink blocks. The simulation is carried out for different cases considering the acceleration mode, constant speed and deceleration mode of electric vehicle.

The DTC based induction motor control method for electric vehicle propulsion system is simple and it has a quick response. As from the simulation results we can conclude that this scheme works effectively in motoring as well as regenerative braking with partial recovery of energy back to the source. As a result, it saves the energy and thus improving the efficiency of the system. Thus the control of IM using this scheme with regenerative braking is a viable option for EV application.

References

[1] M. Ehsani, Y. Gao, S. E.Gay, and A. Emadi,, *Modern Electric, Hybrid Electric and Fuel Cell Vehicles*, CRC press 2005.

ISBN: 978-988-19252-8-2
ISSN: 2078-0958 (Print); ISSN: 2078-0966 (Online)

[2] Mehrdad Ehsani, Khwaja M. Rahman and Hamid A. Toliyat, "Propulsion System Design of Electric and Hybrid Vehicles," *IEEE Tran. On Industrial Electronics* ,Vol.44, Feb 1997.
[3] M. Zeraoulia, M. E. H. Benbouzid and D. Diallo, "Electric motor drive selection issues for HEV propulsion systems: a comparative study", *IEEE Tran. on Industrial Electronics,* Vol.44, No.6, pp.1756-1764, November 2006.
[4] Chang, L.; "Comparison of AC drives for electric vehicles-a report on experts' opinion survey", *Aerospace and Electronic Systems Magazine, IEEE* , vol.9, no.8, pp.7-11, Aug. 1994.
[5] Depenbrock, M., "Direct self control for high dynamics performance of inverter feed AC machines" *ETZArchiv*, Vol. 7, pp.211-218,1985.
[6] Takahashi, I. Noguchi, "A new quick response and high efficiency strategy of an induction motor"*Conf. Rec. IEEE-IAS Annual Meeting*, pp.495-502, 1985.
[7] J. Faiz, M. B. B. Sharifian, Ali Keyhani, and A. B. Proca, "Sensorless Direct Torque Control of Induction Motors Used in Electric Vehicle" *IEEE Trans. Energy Conversion,* Vol.18, No.1, Mar 2003.
[8] J. Faiz, M. B. B. Sharifian, Ali Keyhani, and A. B. Proca,, "Direct Torque Control of Induction Motor for Electric Propulsion Systems" *Electric Power Systems Research,* Vol.51, pp 95-101, Aug 1999.
[9] Bhim Singh, Pradeep Jain, A.P.Mittal, Member and J.R.P.Gupta, "Direct Torque Control: A Practical Approach to Electric Vehicle" *Power India Conference, 2006 IEEE,* Vol.4, 2006.
[10] Singh, B.; Jain, P.; Mittal, A.P.; Gupta, J.R.P, "Speed sensorless electric vehicle propulsion system using DTC IM drive" *Power Electronics, 2006. IICPE 2006. India International Conference on* vol., no., pp.7-11, 19-21 Dec. 2006.
[11] JamesLarminie, John Lowry, *"Electric Vehicle Technology Explained"*, John Wiley and Sons Ltd.
[12] Trovao, J.P.; Pereirinha, P.G.; Jorge, H.M.;"Simulation model and road tests comparative results of a small urban electric vehicle"*Industrial Electronics, 2009. IECON '09. 35th Annual Conference of IEEE*, pp 836-841, 3-5 Nov. 2009
[13] P.C. Krause,*"Analysis of electric Machinery",* McGraw-Hill Book company, 1987.
[14] G. Buja, D. Casadei, and G. Serra,"Direct stator flux and torque control of an induction motor: Theoretical analysis and experimental results" *in Proc. IECON 98, 24th Ann. Conf. IEEE Ind. Electron. Soc*, Vol.1, pp.50-64, 1998.
[15] Peter Vas *"Sensorless Vector and Direct Torque Control"*, Oxford University Press 1998.
[16] Chee Mun ONG *"Dynamic Simulation of Electric Machinery"*, Prentice Hall 1998.
[17] N. R. N. Idris, A.H. M. Yatim, "Direct Torque Control of induction Machines with constant switching frequency and Reduced Torque Ripple " *IEEE Tran. on Industrial Electronics,* Vol.51, No.4, 2004.

ISBN: 978-988-19252-8-2
ISSN: 2078-0958 (Print); ISSN: 2078-0966 (Online)